Dual-azimuth FWI Imaging and its potential in shallow hazard assessment

H. Dinh[1], T. Latter[1], M. Townsend[2], N. Grinde[2]

[1] CGG; [2] Neptune Energy

Summary

High-resolution (HR) site survey acquisitions are traditionally utilized for shallow geohazard investigations and infrastructure planning. However, due to cost reasons, these are often acquired in a sparse 2D manner, and supplemented with conventional multi-streamer 3D seismic imaging aimed at deeper targets. We show how products derived from 100 Hz dual-azimuth (DAZ) full-waveform inversion (FWI) using multi- streamer 3D data, including FWI Imaging, provide a superior uplift in spatial resolution and illumination compared to a combination of both conventional 3D imaging using the same data, and 2DHR site survey data. This is shown to be the case for data and attributes compared against those from a site survey report at various near surface intervals where known geohazards occur. The improved spatial resolution with 100 Hz DAZ FWI can reduce uncertainties in predicting hazards and act as rapidly available supplementary information to a sparser 2DHR survey with less need to acquire a denser 3DHR survey.

Dual-azimuth FWI Imaging and its potential in shallow hazard assessment

Introduction

High interpretation accuracy is required for shallow geohazard analysis prior to drilling and infrastructure placement. 2D single streamer high-resolution (2DHR) seismic surveys are commonly used, which can provide high vertical resolution but inherit 2D acquisition limitations. They are thus susceptible to poor lateral resolution (Douglas, 2011) and limitations in handling out of plane effects, notably diffractions, risking events being imaged incorrectly.

Dense 3D multi-streamer site surveys can be acquired to obtain high-resolution imaging for near surface levels (e.g., Planke et al., 2009). However, these are not often used due to the expense, so a spatially sparse 2DHR site survey may be supplemented with conventional multi-streamer 3D seismic data, with acquisition and imaging aimed at deeper reservoir levels. This may hence lack the required resolution. These problems are exacerbated in shallow water settings, as shown in this work in the Norwegian North Sea (NNS), as much of the primary reflection energy utilized becomes post critical, resulting in a sampling gap deteriorating image accuracy (Bulat & Long, 2006). Furthermore, before being suitable for interpretation, conventional 3D seismic data undergoes a routine of signal processing, extending the cost and turnaround time. This seismic data processing also typically removes multiples, ghosts and diving waves, which contain near surface sampling information that could otherwise improve illumination and imaging.

The aforementioned limitations with both conventional imaging of 3D multi-streamer data and sparse or costly site surveys motivate this work, where Full-waveform Inversion (FWI) Imaging of dual-azimuth (DAZ) conventional multi-streamer data is reviewed as a supplementary dataset for enhanced spatial resolution for shallow hazard assessment with less need for new acquisition. We show that, in the aspects of spatial resolution, the FWI-derived products supersede what can be achieved by a combination of a dedicated 2DHR site survey and conventionally imaged multi-streamer 3D data.

Data Acquisition, Processing and Imaging

The Dugong area is in the NNS, surveyed by two 3D multi-streamer datasets: a North-South oriented variable-depth streamer dataset acquired in 2016, and an East-West oriented multi-sensor dataset obtained between 2020 and 2021. Both datasets have 8 km streamers and 75 m cable separation. These data were most recently processed through a modern DAZ reprocessing and multi-parameter velocity model building flow (Latter et al., 2022), including Time-Lag FWI (TLFWI; Zhang et al., 2018). Furthermore, a 2DHR site survey and associated geohazard report was conducted over the area in 2020, as shown in Figure 1a. This aimed to provide data on bathymetric, seabed and sub-seabed conditions prior to infrastructure placement and drilling operations (Figure 1b) and was supplied for comparative purposes as part of this study.

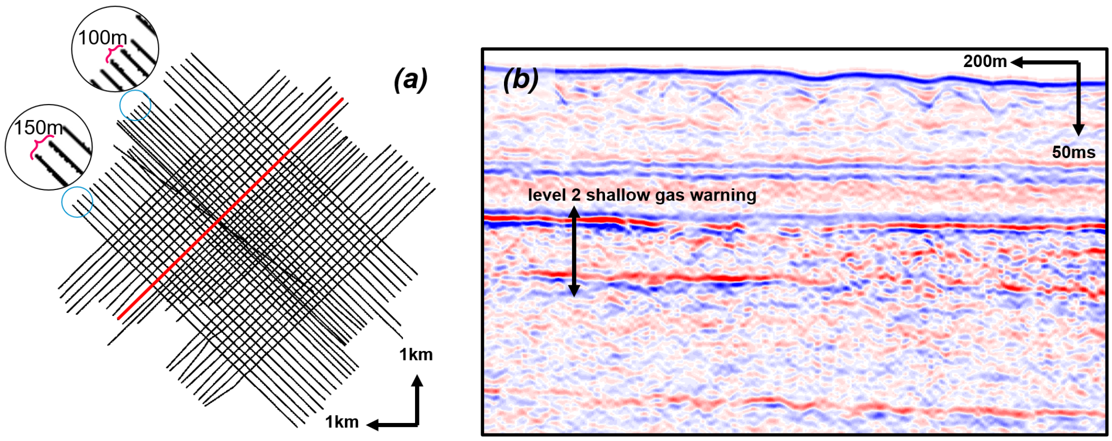

Figure 1 *(a) Layout of the 2DHR site survey with 100 m line separation within a 500 m radius from the well location and 150 m beyond. (b) Cross-section of the red-highlighted line shows high temporal resolution, but spatial resolution is limited between lines. The 429-465 m interval (level 2) was targeted for gas hazard analysis.*

Among the data acquired on the 2DHR survey lines were multibeam echo sounder (MBES). The water depth from MBES was expected to have vertical and horizontal accuracy of 1 m and 2 m, respectively, and a bathymetry map from this data was 3-cell smoothed from a 3 m × 3 m processed size. The processed 2DHR data was initially used to reveal amplitude anomalies possibly associated with shallow gas with supplementary information between the sparse 2D grid provided by a Q-PSDM of the 2016 3D variable depth streamer data to confine the lateral variation of the 2D anomalies. The report indicated warnings of shallow gas bodies in a 429 to 465 m or 552 to 590 ms TWT interval (level 2, Figure 1b).

Methodology

This work employs a 3D DAZ TLFWI inversion that was extended to 100 Hz to achieve a velocity model on a 3.125 x 3.125 m grid with high spatial resolution. It incorporated visco-acoustic (Xiao et al., 2018) and anisotropy terms in the forward modelling. The algorithm utilizes raw data so is available in a short timeframe, and utilizes the full recorded wavefield including diving waves, ghosts, multiples and primary energy, aiming to compensate the near surface spatial sampling limitations of the 2DHR and conventionally primary imaged 3D data. Furthermore, the process employs a least-squares data fitting methodology so improves spatial illumination balancing and signal-to-noise content. The final velocity model then undergoes flexible attribute analyses to obtain:

a. FWI Imaging (Zhang et al., 2020). The product is the reflectivity estimate from the spatial derivative of the velocity volume subject to the given dip θ and azimuth φ of the normal vector n to the subsurface reflector:

$$\partial v/\partial n = \partial v/\partial x * \sin\theta\cos\varphi + \partial v/\partial y * \sin\theta\sin\varphi + \partial v/\partial z * \cos\theta$$

b. Seabed feature map. To derive this, we calculated the seabed interface as the depth at each location at which the maximum derivative value is found:

$$Z_{wb_{x,y}} = argmax\left(\partial v_{x,y}/\partial z\right)$$

The strong contrast between the water layer and the water bottom in most cases was picked up by this argument. However, with an unconsolidated seabed with mixed layers of soft and hard clay stratigraphy, the maximum derivative may represent the boundary between these clay layers. To account for this possible false determination, we replaced the water velocity (considered to be < 1470 m/s) by zero to guarantee the maximum derivative was always the water-seabed contact.

c. Shallow gas hazard map. This was estimated by summing the velocities within the same target interval used in the site survey report (429-465 m) and corrected by the median background sediment velocity $\hat{v}$ in the same interval:

$$A_{x,y} = v_{x,y} - \hat{v}$$

Using an assumption of negative seismic amplitude associated with lower impedance at gas bodies, this method interprets low velocity bodies as gas within the defined interval.

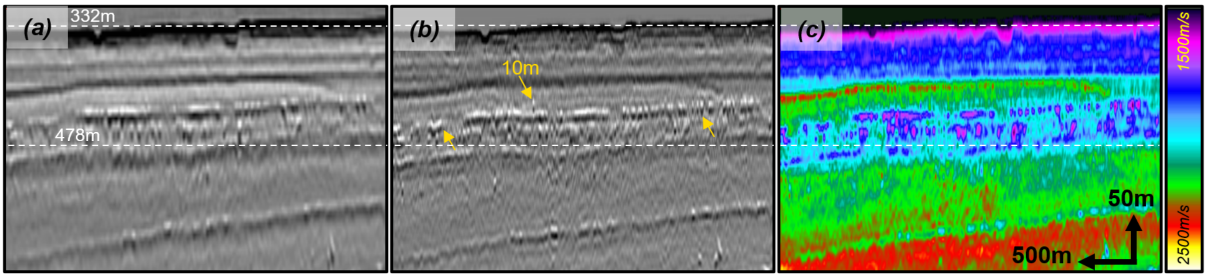

***Figure 2** (a) 3D DAZ Q-Kirchhoff compared to (b) FWI Image derived from (c) 100 Hz 3D DAZ TLFWI. Note significantly improved resolution over the conventional image, delineating gas bodies under 10 m wide. Horizontal dashed lines indicate depth slices shown in Figure 3.*

Results and discussion

Figures 2 and 3 compare images from 100 Hz 3D DAZ TLFWI and the 3D DAZ Q-Kirchhoff migration. Although using an advanced processing and imaging flow (Latter et al., 2022), conventional imaging (Figure 2a) is much lower resolution than the FWI Image from the same acquired data (Figure 2b). Thanks to full-wavefield sampling and the iterative least-squares data fitting process, the DAZ FWI image lateral resolution is superior to the DAZ Q-Kirchhoff (Figures 3b and 3d compared to 3a and 3c, respectively), resolving buried iceberg scour marks (Figures 3e) and small-scale gas accumulations (Figure 3f) of under 10 m width, which were largely invisible on the conventional DAZ imaging.

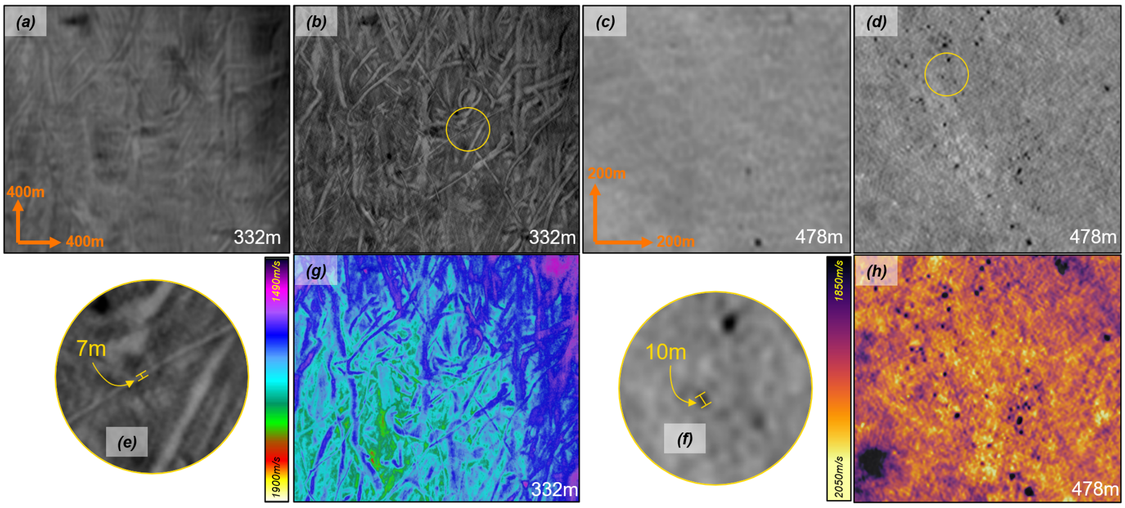

***Figure 3** (a), (c) Conventional DAZ Q-Kirchhoff migration compared to (g), (h) 100 Hz DAZ TLFWI velocities and (b), (d) associated FWI Imaging. Spatial resolution is significantly enhanced with FWI. Zoom reveals finer (e) seabed details and (f) gas hazards in the FWI Image of under 10 m in width.*

Focusing on the seabed bathymetry map derived from the MBES along the 2DHR acquisition lines (Figure 4a) and the FWI-derived map (Figure 4b), it is clear the FWI map has similar characteristics with multidirectional elongated iceberg ploughmarks (green arrows) and numerous depressed pockmarks (shaded circles – yellow arrows). The temporal seabed registration from the FWI-derived map may not be as accurate as MBES, which extends to under 1 m; however, the FWI-derived map using conventional multi-streamer 3D data appears to provide more lateral resolution thanks to the full 3D wavefield inversion and multiple waveform sampling. This in turn potentially resolves missing features not covered by the site survey acquisition grid, such as in areas highlighted by the red arrows.

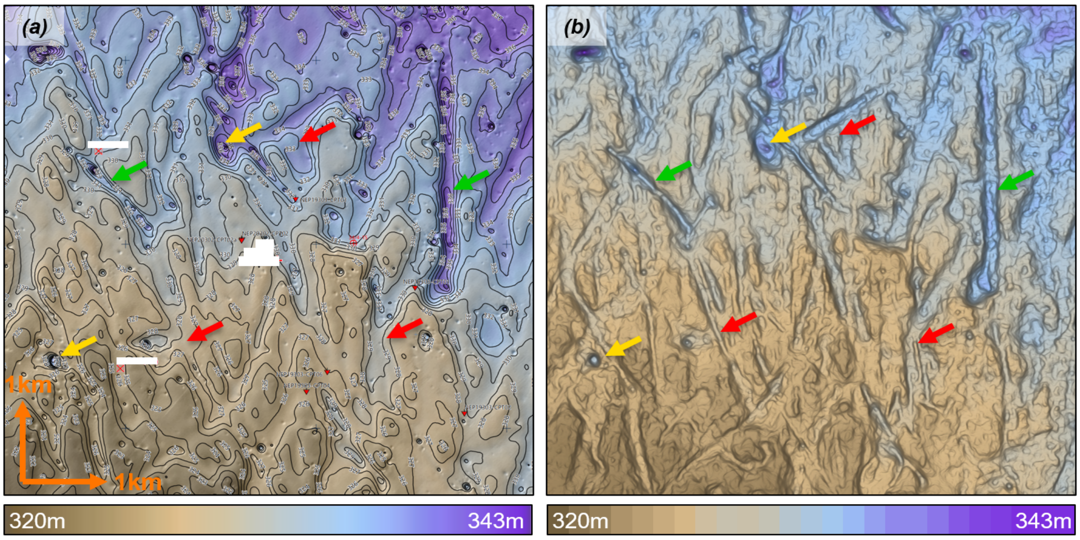

***Figure 4** (a) Site survey bathymetry map shows the seabed with multiple elongated iceberg ploughmarks (green arrows) and shallow pockmarks (yellow arrows). (b) TLFWI maximum derivative map shares similar features but adds enhanced spatial resolution and details (red arrows).*

FWI also provides valuable supplementary information in the interval of interpreted shallow gas hazards in Figure 1b. The derived shallow gas map from the site survey used a combination of prioritised interpretations from the 2DHR data in cyan, and 3D anomalies inferred from a Q-PSDM of conventional multi-streamer data (Figure 5a), which often show low co-location. This mismatch could be due to a combination of the 2D sampling and migration limitations of the 2DHR to image subsurface out-of-plane reflectors, and the low spatial resolution of the conventional 3D imaging. FWI-derived anomalies (Figure 5b), however, are in better correlation to the 2D anomalies from the site survey and significantly improve the resolution of those that could be inferred from the 3D data. This improvement in spatial resolution in a critical interval for drilling hazards could provide enhanced geohazard interpretation and understanding with direct ramifications on infrastructural placement.

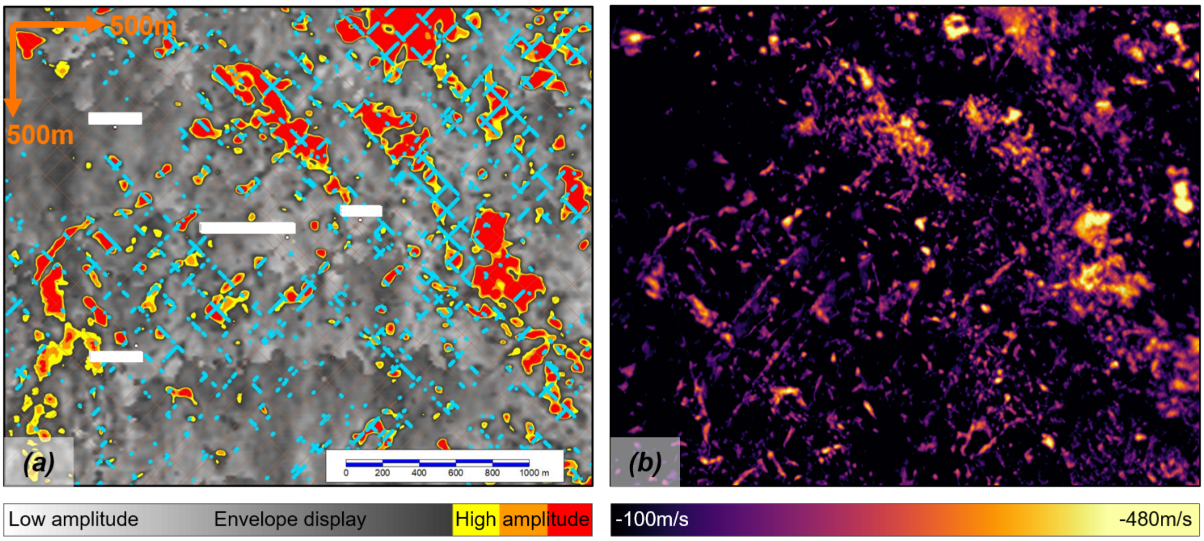

Figure 5 *(a) Site survey amplitude anomaly map: cyan dots are 2DHR interpreted amplitude anomalies, red blobs are amplitude anomalies from 3D multi-streamer Q-PSDM used to provide more information about their lateral variation. (b) Corresponding FWI shallow gas amplitude map shows better spatial resolution and resolves missing features from the site survey data.*

Conclusions

3D DAZ FWI and associated attribute analysis is shown to add value to shallow hazard interpretation in numerous areas. Compared to a 2DHR site survey and conventionally imaged 3D seismic, FWI provides improved spatial resolution and illumination balancing to better delineate scattered gas bodies and other geohazards owing to the full wavefield sampling and least-squares data fitting nature of the process from raw data. FWI Imaging may not replace site surveys owing to the enhanced temporal sampling of 2DHR data, legal or insurance requirements and favourability of survey acquisition timing relative to infrastructural placement decisions, but it is of potential value for rapidly available supplementary analysis, reducing the potential need for more densely sampled 3DHR acquisition.

Acknowledgements

The authors thank CGG Earth Data, Neptune Energy and PL882 partners for their permission to show the data examples and CGG for their permission to publish this work.

References

Bulat, J. and Long, D. [2006] Use of 3D seismic data as a substitute for high-resolution seismic surveys for site investigation. *Health and Safety Executive*.

Douglas, G. [2011] Site survey geophysical acquisition – a recent history and an idealized future. *FORCE geohazards seminar*, Extended Abstract, p. 5.

Latter, T., Gram-Jensen, M., Buriola, F., Dinh, H., Faggetter, M., Jupp, R., Townsend, M., Grinde, N., Machieu, C. and Byerley, G. [2022] The value of dual-azimuth acquisition: imaging, inversion and development over the Dugong area. *83rd EAGE Annual Conference & Exhibition*, Extended Abstracts.

Planke, S., Eriksen, F. N., Berndt, C., Mienert, J. and Masson, D. G. [2009] P-Cable high-resolution seismic. *Oceanography*, **22**(1), 85.

Xiao, B., Ratcliffe, A., Latter, T., Xie, Y. and Wang, M. [2018] Inverting near-surface absorption bodies with full-waveform inversion: a case study from the North Viking Graben in the Northern North Sea. *80th EAGE Annual Conference & Exhibition*, Extended Abstracts, Tu A12 03.

Zhang, Z., Mei, J., Lin, F., Huang, R. and Wang, P. [2018]. Correcting for salt misinterpretation with full-waveform inversion. *88th SEG Annual International Meeting*, Expanded Abstracts, 1143-1147.

Zhang, Z., Wu, Z., Wei, Z., Mei, J., Huang, R. and Wang, P. [2020] Full-wavefield imaging through full-waveform inversion. *90th SEG Annual International Meeting*, Expanded Abstracts, 656-660.